Lumped Parameter Thermal Model of Permanent Magnet Synchronous Machines

Sarah Touhami, Yves Bertin, Yvan Lefèvre, Jean-François Llibre, Carole Hénaux, Matthieu Fénot

LUMPED PARAMETER THERMAL MODEL OF PERMANENT MAGNET SYNCHRONOUS MACHINES

S. Touhami[1],Y. Bertin[2],Y. Lefèvre[1], J. F. Llibre[1], C. Henaux[1], M. Fénot[2]

1. LAPLACE, CNRS, University of Toulouse, Toulouse 31000, France.
2. P' Institute, CNRS, ENSMA, University of Poitiers, UPR 3346, 1 Avenue Clément Ader, BP 40109, 86961 Futuroscope Chasseneuil, France.
e-mail: {stouhami, lefevre, jean-francois.llibre, henaux}@laplace.univ-tlse.fr
{yves.bertin, matthieu.fenot}@ensma.fr

Abstract – This paper describes a thermal equivalent circuit of Liquid Cooling Totally Enclosed Permanent Magnet Synchronous Machines (LCTE-PMSMs). Conductive heat transfer in all directions is taken into account. Specific care has been taken to represent them by equivalent circuit. The conductive heat transfer in heterogeneous media like slots and the convective heat transfer in the airgap and the end-winding are studied.

Keywords – Permanent magnet synchronous machines, thermal equivalent circuit, convection heat transfer, conduction heat transfer, lumped parameter, homogenization, heat sources, thermal conductivity.

1. INTRODUCTION

It is known that excessive temperatures decrease the motor life expectancy. Therefore thermal modeling is very important in the design of electrical machines. According to [1], radiative heat transfer induces in most cases negligible consequences inside the rotating electrical machines. For practical convenience and structural reasons, lumped parameter thermal models are commonly used [1][2]. Theses models are very suitable for conduction phenomena. In radial flux machines where many parts of the machine have cylindrical forms, T-block can be used to model different parts of the machine such as yokes [2]. Nevertheless conduction phenomena are not easily modeled when heteregenous media are involved. For instance, the thermal modeling of slots in electrical machines are still under investigations: according to the purpose of the models several types of thermal models for slot are available [3]-[5]. Lumped parameter models are also used for the modeling of convective heat transfer exchanges in electrical machines. Convection in airgap, end-winding and at end space constitutes a very active research area. In airgap the heat transfer is due to the air flow between the rotor and the stator. Different types of air flow can be distinguished [6][7]:

- smooth airgap without axial flow: this case exists when the electric machine is closed. The flow in airgap is named Taylor-Couette flow,
- smooth airgap with an axial flow combined with rotation of the rotor: in contrast of previous case this configuration exists when the machine is open. The flow in airgap is known as Poiseuille-Taylor-Couette flow,
- slotted airgap with or without axial flow: in this case the flow structure can be similar to Taylor-Couette flow or to Taylor Couette-Poiseuille flow.

Convective and conductive heat transfer studies at end-winding are presented in [8] and [9] respectively. The flow fluid and the convective heat transfer between rotor surface and end-cap surface are studied in [10][11].

This paper will present a thermal model of Liquid Cooling Totally Enclosed Permanent Magnet Synchronous Machines (LCTE–PMSMs). This model takes into account convection and conduction heat transfers in all directions.

2. LUMPED PARAMETER THERMAL MODEL OF PERMANENT MAGNET SYNCHRONOUS MACHINES

One of the methods of thermal study of electrical machines is the nodal approach. This approach is based on a model with an equivalent electrical network of thermal resistances and capacitances. It gives the mean temperatures inside the modeled structure. Fig. 1 shows a radial cut of LCTE–PMSM. In this lumped parameter thermal model, some assumptions are made:

- the structure of the motor is closed,
- bearings are not taken into account in the thermal model,
- shaft is assumed to be non-dissipative,
- motor is assumed symmetric in axial direction; the thermal model of LCTE-PMSM is carried out for middle section,

- conductors in slot are uniformly distributed,
- the slot consists of a group of insulated conductors, surrounded by a main insulation layer,
- only iron losses in stator magnetic core and Joule losses in winding are taken into account in the thermal model given that these losses are the most very important.

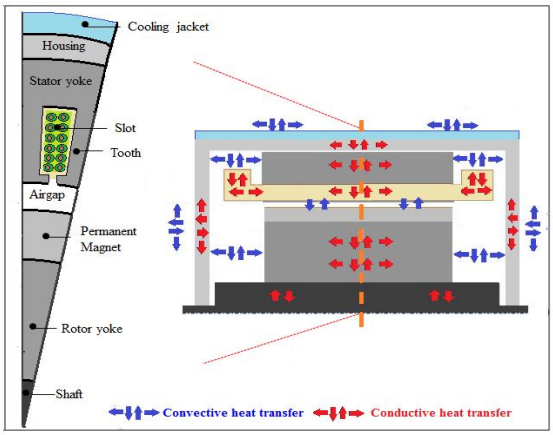

Fig. 1. Radial cut (middle section) of LCTE-PMSM for the thermal modeling [4].

3. HEAT TRANSFER

To study thermal behavior of an electrical machine by modeling, it is required to distinguish three elements: the heat transfer, the heat storage and the heat generation. Heat transfer is generally modeled by thermal resistances of conduction or convection according to heat transfer mechanism. The heat storage is modeled by thermal capacitance. Heat generation is related to losses such as iron and Joule losses.

3.1. CONDUCTION HEAT TRANSFER

A. *Heat conduction equation*

By carrying an energy balance between internal heat produced, heat induced by variation of temperature and which is exchanged in boundaries, equation of heat transfer in isotropy region takes the following form:

$$\rho c_p \frac{\partial T}{\partial t} = p + \mathrm{div}(\lambda \overrightarrow{\mathrm{grad}}(T)) \qquad (1)$$

Where: c_p is the specific heat, ρ is the density, p is the heat generation density, λ is the thermal conductivity and T is the temperature.

B. *Modeling of heterogeneous parts*

In order to take into account thermal aspects of heterogeneous parts of electrical machines such as windings and iron core, one of the methods is to homogenize theses parts and to evaluate equivalent thermal conductivities λ_r^{eq} and λ_a^{eq} respectively in radial and axial directions, equivalent density ρ_e and equivalent specific heat c_{pe}. According to [3]-[5], homogenization formulas used for evaluated radial and axial conductivities, equivalent density and equivalent specific heat are:

- heterogeneous parts with two phases:

$$\begin{cases} \lambda_r^{eq} = \lambda_2 \dfrac{(1+\tau_1)\lambda_1 + (1-\tau_1)\lambda_2}{(1-\tau_1)\lambda_1 + (1+\tau_1)\lambda_2} \\ \lambda_a^{eq} = \sum_i v_i \lambda_i \\ \rho_e = \rho_1 \tau_1 + \rho_2 \tau_2 \\ c_{p_e} = \dfrac{c_{p_1}\tau_1\rho_1 + c_{p_2}\tau_2\rho_2}{\rho_e} \end{cases} \qquad (2)$$

- heterogeneous parts with three phases:

$$\begin{cases} \lambda_r^{eq} = \dfrac{\lambda_2\left[(2\lambda_2+\lambda_1)(\tau_2(2\lambda_2+\lambda_3)+3\tau_1\lambda_1)+3\tau_1\lambda_1(2\lambda_2+\lambda_3)\right]}{\tau_2(2\lambda_2+\lambda_1)(2\lambda_2+\lambda_3)+3\lambda_2(\tau_1(2\lambda_2+\lambda_3)+\tau_3(2\lambda_2+\lambda_1))} \\ \lambda_a^{eq} = \sum_i v_i \lambda_i \\ \rho_e = \rho_1\tau_1 + \rho_2\tau_2 + \rho_3\tau_3 \\ c_{p_e} = \dfrac{c_{p_1}\tau_1\rho_1 + c_{p_2}\tau_2\rho_2 + c_{p_3}\tau_3\rho_3}{\rho_e} \end{cases} \qquad (3)$$

Where τ_1, τ_2, τ_3 are the fill factors (with $\tau_i = S_i/S_{slot}$ $i=1,2,3$ and $\tau_1+\tau_2=1$ for two phases and $\tau_1+\tau_2+\tau_3=1$ for three phases), λ_1, λ_2, λ_3 are the thermal conductivities, c_{p1}, c_{p2}, c_{p3} are the specific heats, v_i is the volume proportion of constituents i in axial direction and λ_i is the thermal conductivity of constituents i.

C. *Thermal Resistance*

For monodimensional conductive heat transfer through solid wall in rectangular geometry (see Fig. 2), thermal resistance is expressed by:

$$R_{cond} = \frac{l}{\lambda S} \qquad (4)$$

Where: l is the thickness of the wall, S is the area of the wall and λ is the thermal conductivity of the wall. For cylindrical geometry with heat transfer, thermal resistances are calculated from equation (1) in cylindrical coordinates (see Fig. 2):

$$\begin{cases} R_1 = \dfrac{1}{2\alpha L\lambda}\left(1 - \dfrac{2r_2^2}{r_1^2 - r_2^2}\ln\left(\dfrac{r_1}{r_2}\right)\right) \\ R_2 = \dfrac{1}{2\alpha L\lambda}\left(\dfrac{2r_1^2}{r_1^2 - r_2^2}\ln\left(\dfrac{r_1}{r_2}\right) - 1\right) \\ R_3 = \dfrac{L}{\alpha\lambda\,(r_1^2 - r_2^2)} \end{cases} \qquad (5)$$

Where: L is the length of cylinder, α is the angle of cylinder part and r_1, r_2 are inner and outer cylinder radius. In the case of cylindrical geometry without heat source, the thermal resistances are given by:

$$\begin{cases} \text{Radial}: R_1 = \dfrac{1}{\alpha L\lambda}\ln\left(\dfrac{r_1}{r_2}\right) \\ \text{Axial} \ : R_2 = \dfrac{L}{\alpha\lambda(r_1^2 - r_2^2)} \end{cases} \qquad (6)$$

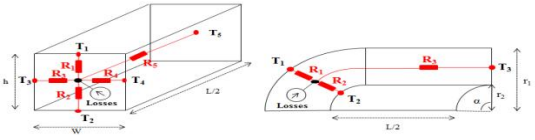

(a) (b)

Fig. 2. (a) Lumped parameter of rectangular geometry (b) Lumped parameter of a hollow cylinder.

D. Thermal capacitance

Some of the heat transferred or produced is stored in the materials of the structure in terms of their mass calorific capacity c_p. The thermal capacitance therefore depends on the type of materials. For a material of volume V, of mass calorific capacity c_p and of density ρ, the thermal capacitance C is equal to:

$$C = c_p \rho V \tag{7}$$

By using equations (4), (5), (6) and (7), we summarized in Table I, the lumped parameter thermal of heat conduction in the different parts of the LCTE-PMSM.

Table I. Lumped Parameter Thermal of Heat Conduction Transfer

Medium	Thermal resistance and capacitance
Slot	$R_{e1}=R_{e2}=h_s/(2\lambda^{eq}_r W_s L_m)$ $R_{e3}=R_{e4}=W_s/(2\lambda^{eq}_r h_s L_m)$ $R_{eax}=L_m/(\lambda^{eq}_a h_s W_s)$ $C_{enc}=c_{pe}\rho_e V$ with: $V=V_{slot}-V_{liner\ slot}$
Liner slot	$R_{ins}=t_{ins}/(S_{ins}\lambda_{ins})$
Tooth	$R_{da}=R_{db}=h_t/(\lambda^{eq}_r W_t L_m)$ $R_{dc}= W_t/(2\lambda^{eq}_r h_t L_m)$ $R_{dax}=2L_m/(\lambda^{eq}_a h_t W_t)$ $C_d=c_{pe}\rho_e V_t$ with: $V_t= L_m h_t W_t/2$
Stator yoke	$R_{culsb}=(1-(2r_2^2/(r_1^2-r_2^2))ln(r_1/r_2))/(2\alpha L_m\lambda^{eq}_r)$ $R_{culsa}=((2r_1^2/(r_1^2-r_2^2))ln(r_1/r_2)-1)/(2\alpha L_m\lambda^{eq}_r)$ $R_{culsax}=L_m/(\alpha\lambda^{eq}_a(r_1^2-r_2^2))$ $C_{culs}= c_{pe}\rho_e V_{culs}$
Housing	Radial:$R_{hra}= ln(r_1/r_2)/(\alpha L\lambda_{al})$ Axial: $R_{hax}= L/(\alpha\lambda_{al}(r_1^2-r_2^2))$ $C_h= c_{pal}\rho_{al}V_{housing}$
End-plate	Radial: $R_{flra}= ln(r_1/r_2)/(\alpha\lambda_{al}t_{end\text{-}plate})$ Axial: $R_{flax}= t_{end\text{-}plate}/(\alpha\lambda_{al}(r_1^2-r_2^2))$ $C_{end\text{-}plate}= c_{pal}\rho_{al}V_{end\text{-}plate}$
Permanent Magnet	$R_{apb}=(1-(2r_2^2/(r_1^2-r_2^2))ln(r_1/r_2))/(2\alpha L_m\lambda_{ap})$ $R_{apa}=((2r_1^2/(r_1^2-r_2^2))ln(r_1/r_2)-1)/(2\alpha L_m\lambda_{ap})$ $R_{apax}=L_m/(\alpha\lambda_{ap}(r_1^2-r_2^2))$ $C_{ap}= c_{pap}\rho_{ap}V_{ap}$
Rotor yoke	$R_{culrb}=(1-(2r_2^2/(r_1^2-r_2^2))ln(r_1/r_2))/(2\alpha L_m\lambda^{eq}_r)$ $R_{culra}=((2r_1^2/(r_1^2-r_2^2))ln(r_1/r_2)-1)/(2\alpha L_m\lambda^{eq}_r)$ $R_{culrax}=L_m/(\alpha\lambda^{eq}_a(r_1^2-r_2^2))$ $C_{culr}= cp_e\rho_e V_{culr}$
Shaft	$C_a= c_{psh}\rho_{sh}V_{sh}$
End-winding	Front part: $R_{ew1a}=R_{ew1b}=L_{ew\text{-}front}/(2\lambda_{cop}k_{fill}h_s W_S)$ $C_{ew1}= c_{pe}\rho_e V_{ew\text{-}front}$ Ring part: $R_{ew2a}=R_{ew2b}= t_{ew\text{-}ring}/(2\lambda^{eq}_r S_{ew\text{-}ring})$ $C_{ew2}= c_{pe}\rho_e V_{ew\text{-}ring}$

3.2. CONVECTION HEAT TRANSFER

A. Convection heat transfer in airgap

For an airgap without axial flow, convective resistance is from the rotor to the stator.The nature of airgap flow depends on modified Taylor number T_{am}, which characterizes the rotation influence. It is evaluated by the following equations [6][7]:

$$T_{am} = \frac{T_a}{F_g} \tag{8}$$

With:

$$T_a = \frac{\Omega^2 R_m e^3}{\upsilon^2} \tag{9}$$

$$F_g = \frac{\pi^4}{P}\frac{1}{1697\,(1-e/2R_m)^2} \tag{10}$$

$$P = 0.0571(1-0.625x)+\frac{0.00056}{1-0.625x} \tag{11}$$

$$x = \frac{e/R_m}{1-e/2R_m} \tag{12}$$

Where: Ω is the rotational speed, R_m is the mean radius, e is the airgap thickness, υ is the kinematic viscosity.

Taking the case where airgap is smooth without axial flow, the flow is [6][7]:

- Stable and laminar when $T_{am} < 1700$,
- Laminar with the appearance of Taylor vortices for $1700 < T_{am} < 10^4$,
- Laminar with Taylor vortices, but the space of evolution changes slightly for $T_{am} > 10^4$.

The flow in airgap is also modeled by the convective heat transfer coefficient h (W.m^{-2}.K^{-1}):

$$h = \frac{\lambda Nu}{D_h} \tag{13}$$

Where: λ is the thermal conductivity. For flow between concentric cylinders such as in the airgap: $D_h=2e$. The nusselt number Nu proposed by "Bercker et Kaye 1962" and used by most authors [1], [2] and [7] are:

$$\begin{cases} Nu = 2 & \text{for} \quad 0 < T_{am} < 1700 \\ Nu = 0.128\ T_{am}^{0.367} & \text{for} \quad 1700 < T_{am} < 10^4 \\ Nu = 0.409\ T_{am}^{0.241} & \text{for} \quad 10^4 < T_{am} < 10^7 \end{cases} \tag{14}$$

B. Convection heat transfer in end-windings

The general empiric formulation of convective heat transfer coefficient given in literature [2][8] is:

$$h = k_1\left(1 + k_2 v^{k_3}\right) \tag{15}$$

Where: v is the speed of air around end-windings, k_1 characterizes natural convection, k_2 and k_3 characterize forced convection and h is the average convective heat transfer coefficient.

Table II. Correlation of Convective Heat Transfer Coefficient Around End-winding

Correlations	k_1	k_2	k_3
[2]	41.4	0.15	1
[3]	15.5	0.29	1
[8]	15.5	0.39	1

C. Convection heat in end cap of rotor

According to [11], the intensity of the air convection heat transfer within the end-space

between the rotor and frame is affected by the speed rotation of the rotor. Due to the high-speed, the flow state of air near the rotor can be turbulent. The flow on the frame surface is laminar. According to [10], the convective heat transfer coefficient on rotor lateral surfaces is calculated by:

$$\begin{cases} Nu = 0.3286\, Re^{0.5} \text{ for } Re < 1.8\times10^5 - 3.5\times10^5 \\ Nu = 0.0196\, Re^{0.8} \text{ for } Re > 2.5\times10^5 - 3.6\times10^5 \\ h = \lambda Nu / D_h \end{cases} \quad (16)$$

Where: Re is the Reynolds number ($Re=r^2\Omega/\nu$), r is the rotor radius and D_h is the hydraulic diameter.

D. Thermal resistance

The convective thermal resistance is defined as:

$$R_{conv} = \frac{1}{hS} \quad (17)$$

Where: S is the surface of convective heat transfer. Table III summarizes the lumped parameter of convection heat transfer.

Table III. Lumped Parameter Thermal of Convection Heat Transfer

Medium	**Thermal resistance and capacitance**
Airgap	$R_g=1/(h_{airgap}\, S_{airgap})$ with $h_{airgap}=\lambda_{air}Nu/(2e)$ $C_g=cp_{air}\rho_{air}V_{air}$
End-winding – Inner air	$R_{tb1}=1/(S_{ew\text{-}ring1}.h_{ew\text{-}ring})$
End-winding – Housing	$R_{tb2}=1/(S_{ew\text{-}ring2}\, h_{ew\text{-}ring})$
Rotor–Inner air	$R_{ina\text{-}rot}=1/(h_{rot}S_{rotax})$
Inner air–End plate	$R_{ina\text{-}plate}=1/(h_{plate}S_{end\text{-}plate})$
Housing–External air	$R_{conv\text{-}hous}=1/(h_{ext}S_{housing})$
End plate–External air	$R_{conv\text{-}plate}=1/(h_{ext}S_{end\text{-}plate})$

Fig. 3 shows the sketch of thermal model of a portion of an angle of representation of LCTE-PMSM. The heat sources come from Joule losses and iron losses of this portion.

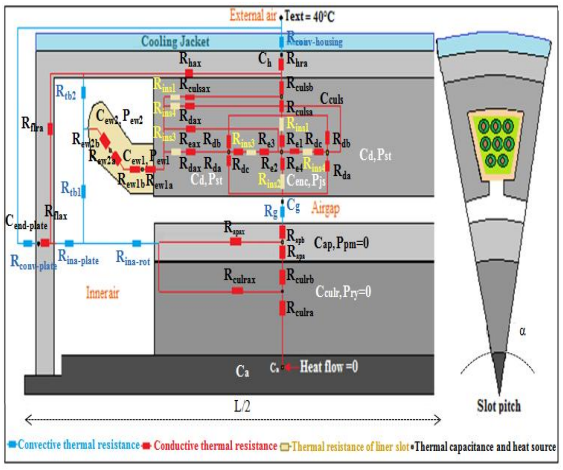

Fig. 3. Sketch of lumped parameter thermal model of LCTE-PMSM.

3.3. HEAT SOURCES

Losses in PMSM constitute the heat sources which contribute to the increase in temperature.The main losses in the PMSMs are the Joule losses in winding and the iron losses in stator magnetic core. They are expressed by the following equations :

- Joule losses

$$P_{joule} = k_{hw}\, \rho\, S_{rot}\, A_{rms}\, J_{rms} \quad (18)$$

Where: k_{hw} is the head winding coefficient (ratio between the length of half turn and the active length), ρ is the electric resistivity, S_{rot} is the external rotor surface, A_{rms} is the linear current density and J_{rms} is the current density.

- Iron loss (Bertotti's model) [10]

$$P_{Iron} = k_h\, fB_m^2 + k_c\,(fB_m)^2 + k_e\,(fB_m)^{1.5} \quad (19)$$

Where: k_h is the hysteresis loss coefficient, k_c is the eddy current coefficient, k_e is the excess loss coefficient, f is the frequency and B_m is the maximum magnetic induction.

3.4. LUMPED PARAMTER THERMAL MODEL RESULTION

The lumped parameter thermal model (Fig. 3) presented with N Nodal temperatures, can be expressed with energy balance for each node:

$$[C]\frac{d[T]}{dt} = [R]^{-1}[T] + [P] \quad (20)$$

Where: [T] is the temperature vector, [C] is the thermal capacitance matrix, [R] is the thermal resistance matrix, and [P] is the heat source vector.

Using Kirchhoff's circuit laws, the resolution of lumped parameter thermal model can be simplified by equation (21).

$$[C]\frac{d[T]}{dt} = [I][R]^{-1}[I]^t[T] - \left([P] - [I][R]^{-1}[V]^t T_{ext}\right) \quad (21)$$

Where: [I] is the incidence matrix and [V] is the incidence vector for reference node which represented by the ambient air temperature T_{ext}.

4. APPLİCATİON

The report of T. A. Burress in [11] publishes detailed data of hybrid electric vehicle (HEV) in 2011. In this report, the Lexus LS600h has the highest specific power of 2.46kW/kg. Taking this example, a PMSM with a specific power of 3kW/kg with the same rated power and speed as the Lexus LS 600h has been sized using Slemon's model [12]. Tables IV, V and VI give the sizes of the motor, the heat sources of the thermal model and the material thermal properties. Table VII shows heat transfer coefficients that must be imposed in order to have the winding temperature within acceptable range: 120°C-130°C.

This result shows that for a PMSM with 3kW/kg the heat transfer coefficients are already large compared to those found in literature [2] and [13] for indusrial motors.

A second PMSM with a specific power of 5kW/kg and the same rated power has been also sized. In order to reach this last specific power, the speed, the tangential stress and some other assumptions must be changed (see Table IV). Table V shows the new values of heat sources. Necessary heat transfer coefficients to have winding temperature within acceptable range are given in Table VII. It can be noticed that the heat transfer coefficient of the housing external surface has to be increased of about 50%.

Table IV. Main Dimensions and Parameters of LCTE-PMSM

Motor part		**PMSM 3kW/kg**	**PMSM 5kW/kg**
Power	P [kW]	110	110
Speed	N [rpm]	4500	5500
Number of poles	$2p$	8	8
Number of slots	N_s	48	48
Number of phases	q	3	3
Tangential stress	σ_t [kPa]	85	148.5
Current density	j[A/mm²]	12	12
Max airgap flux density	B_{gm}[T]	1.02	1.02
Tooth flux density	B_t [T]	1.5	1.8
Yoke flux density	B_y [T]	1.5	1.8
Outer frame radius	R_f[mm]	119.18	102.65
Outer stator yoke radius	R_y[mm]	107.7	92.26
Inner stator radius	R_s[mm]	59.21	45.98
Active length	L_m[mm]	124.6	96.80
Frame length	L[mm]	174.4	135.5
Yoke height	h_y[mm]	10.06	6.51
Slot height	h_s[mm]	38.48	39.76
Slot width	W_s[mm]	4.4	3.8
Tooth width	W_t [mm]	3.4	2.2
Airgap thickness	e [mm]	1.18	0.92
PM thickness	t_{pm}[mm]	4.19	3.25
Shaft radius	R_{sh}[mm]	43.77	35.3
Motor weight	W_{mot} [kg]	35.34	21.33
Total Joule losses	P_j [kW]	2.651	2.793
Total Stator Iron losses	P_{iron}[W]	541.2	475.3

Table V. Heat Sources of Lumped Parameter Thermal Model of LCTE-PMSM

Motor part		**PMSM 3kW/kg**	**PMSM 5kW/kg**
Stator Slot	P_{js} [W]	19.73	20.79
End-winding: front part	P_{ew1}[W]	3.80	5.31
End-winding: ring part	P_{ew2}[W]	4.09	3.01
Stator yoke	P_{sy}[W]	2.89	2.32
Stator tooth	P_{st}[W]	2.76	2.64
Permanent Magent	P_{PM}[W]	Neglected	Neglected
Rotor yoke	P_{ry}[W]	Neglected	Neglected

Table VI. Thermophysical properties of materials used in LCTE-PMSMs

Material	**thermal conductivity** [W/(m.K)]	**specific heat** [kJ/kg.K]	**density** [kg/m^3]
Vacoflux48	rad/tang : 46 axial : 0.6	0.46	8120
Copper	360	0.39	8920
Sm_2Co_{17}	10	0.35	8300
Aluminum	209	0.9	2700
Stainless	17	0.465	7900
Air	0.025	1	1.177
Epoxy	0.5	-	1500
LordSC320	3.2	-	-

Table VII. Convection Heat Transfer Coefficients

Convection heat transfer [W/(m².K)]		**PMSM 3kW/kg**	**PMSM 5kW/kg**
Housing	h_{ext}	222.1	340
Airgap	h_{airgap}	66.8	74
Rotor–Inner air	h_{rot}	22.6	25
End-plates-Inner air	h_{plate}	10	10
End-winding	$h_{ew\text{-}ring}$	130	130

The simulation results of lumped parameter thermal model of LCTE-PMSMs are shown in Fig. 4. The temperatures of the hot media such as the slot and the end-winding remain above 130°C for LCTE-PMSM with specific power of 3kW/kg and greater than 150°C for LCTE-PMSM with specific power of 5kW/kg. A large part of the losses is evacuated through the cooling system placed on the surface housing by forced convection and a small part of losses is evacuated by natural convection through the end-plate. Therefore, for a specific power of 5kW/kg, the cooling effort must be further improved in order to have an acceptable temperature in the winding (see convection heat transfer values h_{ext} in Table VII). Results on Fig.4 can help to determine where the cooling effort must be done.

CONCLUSION

The thermal model described in this paper is an improvement of the calculation of lumped parameters for a Liquid Cooling Totally Enclosed Permanent Magnet Synchronous Machine (LCTE-PMSM). It takes into account conductive heat transfer in slots and teeth, stator and rotor yokes, end-windings and permanent magnets. It also takes into account convective heat transfer in airgap, housing, end-plates, end-windings, inside and outside of the machine. The main heat sources considered in this study are Joule and iron losses. The studied applications show one of the uses of the proposed approach: evaluation of the cooling effort to be done in order to reach a given level of specific power.

ACHNOWLEDGEMENT

This project has received funding from the [European Union's Horizon 2020 (Cleansky 2JTI) research and innovation programme, 2014-2024] under grant agreement No 715483.

REFERENCES

[1] J. Nerg, M. Rilla, J. Pyhönen, Thermal Analysis of Radial-Flux Electrical Machines with a High Power Density, IEEE Trans. On Industrial Electronics, vol. 55, no. 10, pp. 3543-3554, October 2008.

[2] A. Boglietti, A. Cavagnino, Analysis of the End winding Cooling Effects in TEFC Induction Motors, IEEE Trans. On Industry Applications, vol. 43, no. 5, pp.1214-1222, Sept 2007.

[3] A. Boglietti, A. Cavagnino, M. Lazzari, M. Pastorlli, A simplified thermal model for variable speed self-cooled induction motor, IEEE Trans. On Industry Applications, vol. 39, no. 4, pp.945-952, July/August 2003.

[4] A. Fasquelle, Contribution à la modélisation multi-physique: électro-vibro acoustique aérothermique de machines de traction, PhD thesis, Ecole Central de Lille, 30 November 2007.

[5] M. Fénot, Y. Bertin, E. Dorignac, G. Lalizel, A review of heat transfer between concentric rotating cylinders with or without axial flow, International Journal of Thermal Sciences, Elsevier, vol. 50, issue 7. pp. 1138–1155, July 2011.

[6] D. A. Howey, Peter R.N. Childs, A. S. Holmes, 'Air-gap convection in rotating electrical machines', IEEE Trans. On Industrial Electronics, vol. 59, no.3, March 2012.

[7] L. Idoughi, X. Mininger, F. Bouillault, L. Bernard and E. Hoang, Thermal Model with winding Homogenization and FIT Discretization for Stator Slot, IEEE Trans. On Magnetics, vol. 47, no. 12, pp.4822-4826, December, 2011.

[8] P. H. Mellor, D. Roberts, D.R. Turner, Lumped parameter thermal model for electrical machines of TEFC design, IEE Proceedings-B, vol. 138, no. 5, September 1991.

[9] B. Zhang, R. Qu, J. Wang, W. Xu, X. Fan, Y. Chen, Thermal model of totally enclosed water-cooled permanent magnet synchronous machines for electric vehicle application, IEEE Trans. On Industry applications, vol. 51, no. 4, pp. 3020-3028 July/August, 2015.

[10] G. Bertotti, General Properties of Power Losses in soft Ferromagnetic Materials, IEEE Trans. On Magnetics, vol. 24, no. 1, pp. 621-630, January 1988.

[11] T. A. Burress et al, Evaluation of the 2010 Toyota Prius Hybrid Synergy Drive System, Technical Report of Oak Ridge National Laboratory,March2011,https://www.osti.gov/scitech/biblio/1007833.

[12] G. R. Slemon, On the Design of High-Performance Surface-Mounted PM Motors, IEEE Trans. On Industry Applications, vol. 30, no. 30, pp.134-140, January/February, 1994.

[13] D. A. Staton, A. Cavagnino, Convection heat transfer and flow calculations suitable for electric machines thermal models, IEEE Trans. On Industrial Electronics, vol. 55, no. 10, pp.3509-3516, October 2008.

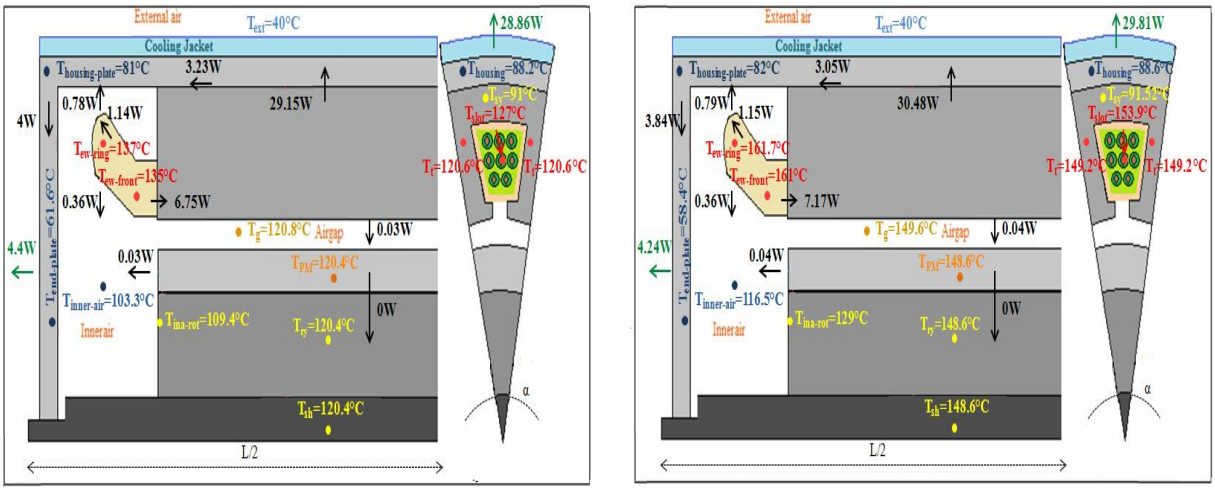

(a) (b)

Fig. 4. Temperatures and heat flows (a) 3kW/kg LCTE-PMSM (b) 5kW/kg LCTE-PMSM